Biochimica et Biophysica Acta 1848 (2015) 3188–3196

Contents lists available at ScienceDirect

Biochimica et Biophysica Acta

journal homepage: www.elsevier.com/locate/bbamem

VDAC3 gating is activated by suppression of disulfide-bond formation between the N-terminal region and the bottom of the pore

Masateru Okazaki [a,b], Katsue Kurabayashi [a,b], Miwako Asanuma [a,b], Yohei Saito [a,b], Kosuke Dodo [a,b], Mikiko Sodeoka [a,b,*]

[a] Sodeoka Live Cell Chemistry Project, ERATO, JST, 2-1 Hirosawa, Wako, Saitama 351-0198, Japan
[b] Synthetic Organic Chemistry Laboratory, RIKEN, 2-1 Hirosawa, Wako, Saitama 351-0198, Japan

ARTICLE INFO

Article history:
Received 2 March 2015
Received in revised form 9 September 2015
Accepted 18 September 2015
Available online 25 September 2015

Keywords:
Voltage-dependent anion channel
Recombinant protein
Planar lipid bilayer
Disulfide-bond
S-nitrosylation
Redox sensing

ABSTRACT

The voltage-dependent anion channels (VDACs), VDAC1, VDAC2, and VDAC3, are pore-forming proteins that control metabolite flux between mitochondria and cytoplasm. VDAC1 and VDAC2 have voltage-dependent gating activity, whereas VDAC3 is thought to have weak activity. The aim of this study was to analyze the channel properties of all three human VDAC isoforms and to clarify the channel function of VDAC3. Bacterially expressed recombinant human VDAC proteins were reconstituted into artificial planar lipid bilayers and their gating activities were evaluated. VDAC1 and VDAC2 had typical voltage-dependent gating activity, whereas the gating of VDAC3 was weak, as reported. However, gating of VDAC3 was evoked by dithiothreitol (DTT) and *S*-nitrosoglutathione (GSNO), which are thought to suppress disulfide-bond formation. Several cysteine mutants of VDAC3 also exhibited typical voltage-gating. Our results indicate that channel gating was induced by reduction of a disulfide-bond linking the N-terminal region to the bottom of the pore. Thus, channel gating of VDAC3 might be controlled by redox sensing under physiological conditions.

1. Introduction

The voltage-dependent anion channels (VDACs), which are localized in the mitochondrial outer membrane, are pore-forming proteins that control the flux of metabolites between mitochondria and cytoplasm (reviewed in [1]). Their conformational states are voltage-dependent and exhibit different selectivities and permeabilities for small ions, showing a preference for anions in the open state and for cations in the closed state [2]. VDACs also play crucial roles in various cellular processes, including the transfer of ADP and ATP [3], reactive oxygen species (ROS) signaling [4], anchoring of hexokinases [5], and apoptosis mediated by release of cytochrome c [6] or interaction with Bcl-2 family members [7]. In mammals, the VDAC protein family consists of three isoforms: VDAC1, VDAC2, and VDAC3. All VDAC isoforms are highly expressed in heart, kidney, brain and skeletal muscle, but only VDAC2 and VDAC3 are expressed in testes, especially in outer dense fibers [8]. VDACs exist in mitochondrial outer membrane [9]. VDAC1 and VDAC2 are co-localized predominantly within the same restricted area in the outer membrane, while VDAC3 is broadly distributed over the surface of the mitochondrion [10]. The amino acid sequences of the three human VDAC isoforms show approximately 70% identity. Phylogenetic analysis indicated that VDAC3 might be evolutionarily distinct, and thus might have a different physiological function from the others [11]. VDAC3 plays roles in sperm motility by microtubule doublet formation [12] and in ciliary disassembly in cycling cells by targeting Mps1 protein kinase to centrosomes [13,14]. Overexpression of human VDAC isoforms in yeast strains lacking endogenous porin 1 gene revealed that VDAC3 has a very weak protective activity against ROS, unlike the other isoforms [4]. Moreover, channel gating of VDAC3 was rarely observed in an artificial planar lipid bilayer [15,16], suggesting this isoform did not exhibit typical voltage-dependent channel gating.

On the other hand, it was reported that VDAC3-deficient cancer cells showed reduced permeability for ADP/ATP, as well as dramatically decreased mitochondrial membrane potential (MMP) [17,18]. It was unclear how VDAC3 could exhibit such behavior if it has poor channel gating activity. One possibility is that VDAC3 is activated by post-translational modification for proper functioning. Indeed, many post-translational modifications of VDACs, such as phosphorylation [19], acetylation [20], tyrosine nitration [21], S-nitrosylation [22,23], and ubiquitination [24] have been reported. Recently, it was also reported that swapping of the N-terminal region of VDAC3 with that of VDAC1 greatly increased the channel activity [16,25]. This suggested that

Abbreviations: VDAC, voltage-dependent anion channel; LDAO, *n*-dodecyl-*N*,*N*-dimethylamine-*N*-oxide; CV, column volume; DTT, dithiothreitol; IAA, iodoacetamide; GSNO, *S*-nitrosoglutathione; ROS, reactive oxygen species; MMP, mitochondrial membrane potential; SDS-PAGE, sodium dodecyl sulfate-polyacrylamide gel electrophoresis; TCA, trichloroacetic acid; NO, nitric oxide

* Corresponding author.
E-mail address: sodeoka@riken.jp (M. Sodeoka).

http://dx.doi.org/10.1016/j.bbamem.2015.09.017

cysteine residues at the N-terminal region might be important, because VDAC3 has two cysteines but VDAC1 has no cysteine in this region. Based on these results, we hypothesized that VDAC3 is activated by cysteine modification.

In this work, we expressed the human VDAC isoforms in bacterial systems and examined their electrophysiological properties and gating activity in artificial planar lipid bilayers. We further investigated the molecular mechanism of activity regulation by examining the effects of dithiothreitol (DTT) and *S*-nitrosoglutathione (GSNO), which are expected to suppress disulfide-bond formation, as well as the effect of mutation of N-terminal cysteine residues, on the channel gating properties of VDAC3.

2. Materials and methods

2.1. Expression, purification, and refolding of recombinant human VDAC proteins

cDNAs for human voltage-dependent anion channels 1, 2, and 3, corresponding to GeneBank accession numbers BC008482.1, BC012883.1, and BC056870.1, were cloned into multiple cloning sites of the pET21d vector (Novagen) with a C-terminal His_6-tag. The deduced amino acid sequences of VDAC-His_6 proteins are shown in Fig. 1. After DNA sequencing, each VDAC protein was expressed in *Escherichia coli* BL21 (DE3) cells in the presence of 1 mM IPTG and 0.2% L-arabinose at 37 °C overnight. The bacterial cells were suspended in suspension buffer (20% sucrose, 0.6% Triton-X 100, 5 μg/mL lysozyme, 1 μM phenylmethylsulfonyl fluoride, 3.8 nM aprotinin, and 50 nM leupeptin) and lysed by sonication on ice. Inclusion bodies containing VDAC were dissolved in a resuspension buffer (50 mM Tris (pH 8.0), 100 mM NaCl, 6 M guanidine-HCl) and sonicated. After centrifugation, a quarter amount of a dilution buffer (50 mM Tris–HCl (pH 8.0), 100 mM NaCl) was added to the supernatant, followed by His-tag affinity purification and on-column refolding according to the reported method [26,27]. A denatured sample was loaded onto a Ni-NTA agarose (QIAGEN) packed column pre-equilibrated with 5 column volumes (CVs) of a wash buffer (50 mM Tris (pH 8.0), 100 mM NaCl, 4.5 M guanidine-HCl). The column was washed with 5 CVs of a wash buffer followed by 5 CVs of a low-imidazole wash buffer (50 mM Tris (pH 8.0), 100 mM NaCl, 4.5 M guanidine-HCl, 25 mM imidazole). VDAC proteins were refolded on a column in 5 CVs of a refolding buffer (50 mM Tris (pH 8.0), 100 mM NaCl, 0.4% *n*-dodecyl-*N*,*N*-dimethylamine-*N*-oxide (LDAO, Affymetrix) provided as powder) and eluted with an elution buffer (50 mM Tris (pH 8.0), 100 mM NaCl, 0.4% LDAO, 500 mM imidazole). The eluate was dialyzed against 100 volumes of a dialysis buffer (25 mM $NaPO_4$ (pH 7.0), 1 mM EDTA, 1 mM dithiothreitol (DTT), 0.1% LDAO) with a 8000 MWCO dialysis membrane two times for 1 h and additional one for 1 day. Cation-exchange chromatography was performed for further purification. The samples were loaded onto a 1 mL RESOURCE™ S column (GE Healthcare) equilibrated with a wash buffer (25 mM $NaPO_4$ (pH 7.0), 5 mM DTT, 0.1% LDAO) using ÄKTA explorer 10S (GE Healthcare). VDAC proteins were eluted with a 10–16% gradient formed with an elution buffer (25 mM $NaPO_4$ (pH 7.0), 5 mM DTT, 0.1% LDAO, 1 M NaCl) and the concentration was determined using absorption at 280 nm. The purified proteins were also analyzed by SDS-PAGE and immunoblotting using commercially available antibodies against VDAC1 (SantaCruz Biotechnology, sc8828) and VDAC2 (Proteintech, 11663-AP), and an anti-VDAC3 antibody (SCRUM Inc.) directed against a synthetic VDAC3-specific amino acid sequence (SVFNKGYGFM) [8].

2.2. Electrophysiological monitoring

Electrophysiological properties of VDACs were monitored using an Ionovation Compact (Ionovation), which is a bench-top bilayer formation system based on the painting method [28]. An artificial planar lipid bilayer was formed on an aperture of about 50 μm diameter in a 25 μm thick Teflon foil separating the *cis*- and *trans*-chambers filled with the buffer (250 mM KCl, 2 mM $CaCl_2$, 10 mM MOPS-Tris (pH 7.0)). The chambers were connected to the amplifier via Ag/AgCl-electrodes with 1 M KCl salt bridges. Bilayer formation was carried out by addition of 5 mg/mL of Ionovation bilayer lipid II: POPE/POPC = 8/2 (Ionovation), which was dissolved in *n*-decane, to the *trans*-chamber (ground electrode), monitored optically by a CCD camera. Ionovation Compact monitors the capacitance change in real-time during the membrane formation process, and use it as an indicator for membrane formation. More than 50 pF of membrane capacitance was accepted for proper lipid bilayers. After bilayer formation, VDAC proteins were applied to the *cis*-chamber (signal electrode). The currents were acquired with a sampling frequency of 10 kHz after low-pass-filter at 3 kHz, and digitized using an EPC 10 Patch Clamp Amplifier and Patchmaster software (HEKA). Electrophysiological channel properties were monitored under a symmetrical 0.5 kHz triangular voltage wave of ±50 mV. Conductance was calculated by the use of the following equation: conductance (G) = current (I)/voltage (V).

2.3. Electrophysiological monitoring of VDAC3 in reducing conditions

Firstly, channel gating of VDAC3 was monitored in the presence of 5 mM DTT (Sigma-Aldrich) to see whether reducing conditions affect the channel properties. Secondly, to determine whether disulfide-bond formation is involved, cysteine residues of VDAC3 were alkylated with 1 μM iodoacetamide (IAA, Wako) at 30 °C for 30 min and the

VDAC1
MAVPPTYADL GKSARDVFTK GYGFGLIKLD LKTKSENGLE FTSSGSANTE TTKVTGSLET
KYRWTEYGLT FTEKWNTDNT LGTEITVEDQ LARGLKLTFD SSFSPNTGKK NAKIKTGYKR
EHINLGCDMD FDIAGPSIRG ALVLGYEGWL AGYQMNFETA KSRVTQSNFA VGYKTDEFQL
HTNVNDGTEF GGSIYQKVNK KLETAVNLAW TAGNSNTRFG IAAKYQIDPD ACFSAKVNNS
SLIGLGYTQT LKPGIKLTLS ALLDGKNVNA GGHKLGLGLE FQALEHHHHH H

VDAC2
MASMTGGQQM GRIRIHMATH GQTCARPMCI PPSYADLGKA ARDIFNKGFG FGLVKLDVKT
KSCSGVEFST SGSSNTDTGK VTGTLETKYK WCEYGLTFTE KWNTDNTLGT EIAIEDQICQ
GLKLTFDTTF SPNTGKKSGK IKSSYKRECI NLGCDVDFDF AGPAIHGSAV FGYEGWLAGY
QMTFDSAKSK LTRNNFAVGY RTGDFQLHTN VNDGTEFGGS IYQKVCEDLD TSVNLAWTSG
TNCTRFGIAA KYQLDPTASI SAKVNNSSLI GVGYTQTLRP GVKLTLSALV DGKSINAGGH
KVGLALELEA LEHHHHHH

VDAC3
MCNTPTYCDL GKAAKDVFNK GYGFGMVKID LKTKSCSGVE FSTSGHAYTD TGKASGNLET
KYKVCNYGLT FTQKWNTDNT LGTEISWENK LAEGLKLTLD TIFVPNTGKK SGKLKASYKR
DCFSVGSNVD IDFSGPTIYG WAVLAFEGWL AGYQMSFDTA KSKLSQNNFA LGYKAADFQL
HTHVNDGTEF GGSIYQKVNE KIETSINLAW TAGSNNTRFG IAAKYMLDCR TSLSAKVNNA
SLIGLGYTQT LRPGVKLTLS ALIDGKNFSA GGHKVGLGFE LEALLEHHHH HH

Fig. 1. Deduced amino acid sequences of VDAC-His_6 proteins. The underlined characters show additional sequence tags derived from pET21d. Bold characters in the VDAC3 sequence show cysteine residues, which were mutated to alanine in mutation analysis.

electrophysiological channel properties were monitored in the absence of DTT. Finally, channel gating of VDAC3 was monitored in the presence of 1 mM GSNO (Merck) to examine the possible physiological function of VDAC3.

2.4. SDS-PAGE analysis of the oxidized VDAC3 proteins

The reduced and oxidized forms of VDAC3 were analyzed by non-reducing SDS-PAGE. To prevent the oxidation of free cysteine residues during the SDS-PAGE operations, cysteine residues of VDAC3 were alkylated before loading to the gel. After dilution or addition of H_2O_2, the recombinant VDAC3-His_6 solution (final concentration was 40 nM) was incubated with 100 μM IAA at RT for 10 min. The protein samples were precipitated using 20% ice-cold trichloroacetic acid (TCA), washed with ice-cold acetone, and solubilized in a phosphate buffer (pH 7.0). Solubilized samples were subjected to non-reducing SDS-PAGE and analyzed by immunoblot using generated anti-VDAC3 antibody.

2.5. Site-directed mutagenesis

Cysteine residues of VDAC3 in the expression vector pET21d were mutated to alanine using a QuikChange Site-Directed Mutagenesis Kit (Agilent Technologies) according to the manufacturer's protocol. Point mutations at Cys2, Cys8, Cys36, Cys65, Cys122, Cys229, and at both Cys2 and Cys8 (cysteine residues of VDAC3 are shown in bold characters in Fig. 1) were designated as C2A, C8A, C36A, C65A, C122A, C229A, and C2A/C8A, respectively.

2.6. Homology modeling

A homology model of VDAC3 was constructed by MODELLER 9v1 [29] using the reported crystal structure of VDAC1 (PDB ID: 3EMN [30]). The images were drawn by PyMOL software.

3. Results

3.1. Purification of bacterially expressed human VDAC proteins

Expressed human VDAC proteins were solubilized from inclusion bodies under denaturing conditions and refolded by means of the on-column refolding method. The final concentrations of purified VDAC proteins were as follows: VDAC1, 1.2 mg/mL; VDAC2, 0.7 mg/mL; and VDAC3, 0.6 mg/mL. SDS-PAGE analysis showed that the three isoforms, VDAC1-His_6, VDAC2-His_6, and VDAC3-His_6, each gave a single major band (Fig. 2A). Their estimated molecular weights were 31,838, 34,388, and 31,837, respectively, although the migration of VDAC3-His_6 was slightly faster than that of VDAC1-His_6. Nevertheless, immunodetection by anti-VDAC antibodies directed against each VDAC isoform confirmed that the detected bands reacted with the specific antibodies (Fig. 2B). Hence, all recombinant human VDAC proteins were successfully purified.

3.2. Electrophysiological properties of VDAC isoforms

Detergent-solubilized VDAC1-His_6, VDAC2-His_6, and VDAC3-His_6 were incorporated into planar lipid bilayers and current traces under applied voltage were recorded to monitor their gating activities. Single-channel monitoring showed that VDAC1 and VDAC2 gated in response to linearly changing voltage, while VDAC3 did not respond well (Fig. 3A). The ratio of the conductance at applied voltage (G) to maximum conductance (G_{max}) showed a symmetrical, bell-shaped distribution for VDAC1 and VDAC2, though voltage dependency of VDAC2 was weaker than VDAC1 (Fig. 3B). In the case of VDAC3, the slope was very shallow, indicating the channel rarely gate depending on voltage. Histogram of maximum conductances indicated that open state conductances of VDAC1 and VDAC2 were in a range between 1.25–1.5 nS (at 250 mM KCl) (Fig. 3C). On the other hand, VDAC3 showed lower conductance states.

3.3. Activation of channel gating of VDAC3 in reducing conditions

Poor voltage-dependent gating activity of VDAC3 has already been reported, but the reason for the low activity, in spite of high sequence similarity of VDAC3 with VDAC1 and VDAC2, remains unclear. Since the regular buffer solution for electrophysiological experiments does not contain DTT, we suspected that cysteine residues in VDAC3 might be in oxidized form under the experimental conditions. Since VDAC3 contains as many as 6 cysteines, we speculated that disulfide-bond formation might account for the low activity. To examine this possibility, the voltage-gating properties of VDAC3 were monitored in the presence of 5 mM DTT. As we anticipated,

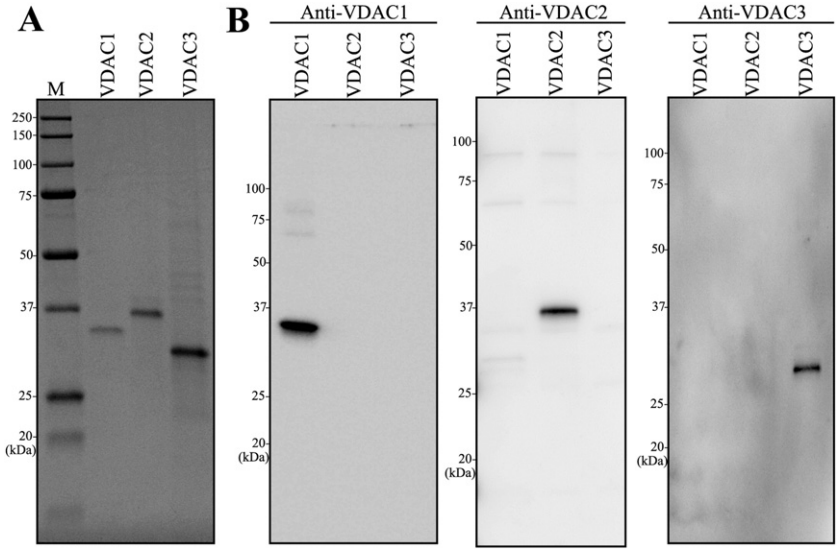

Fig. 2. Purification of bacterially expressed VDAC-His_6 proteins. (A) SDS-PAGE of recombinant purified VDAC1-His_6, VDAC2-His_6, and VDAC3-His_6. Lane M shows molecular size markers. (B) Immunodetection of the recombinant purified VDAC proteins using anti-VDAC antibodies against VDAC1, VDAC2, and VDAC3.

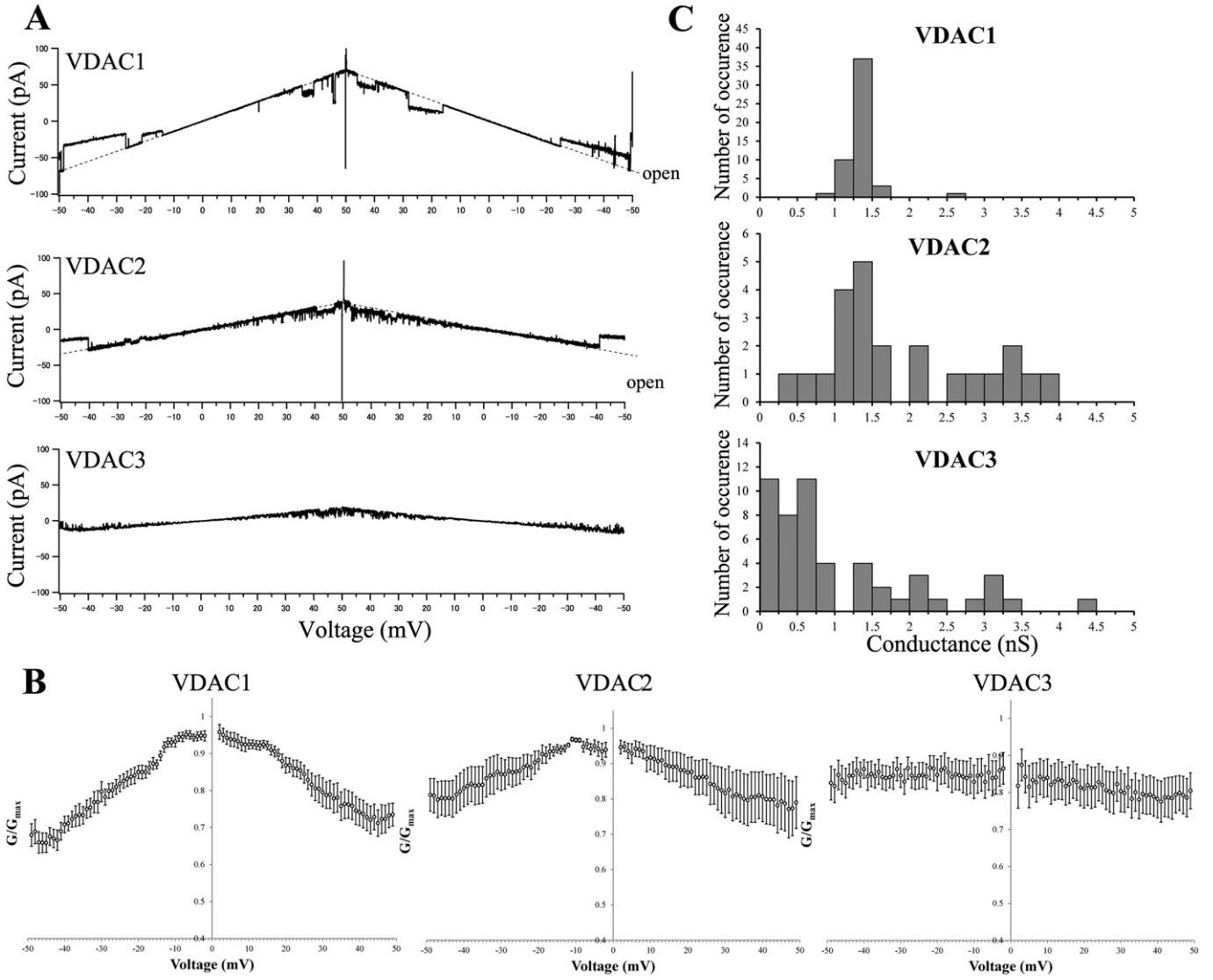

Fig. 3. Difference of voltage-gating processes between VDAC channels. (A) Representative current traces of VDAC channels under triangular voltage waves (±50 mV, 0.5 kHz). Final concentrations of VDAC-His_6 proteins were in a range of 0.1–10 ng/each chamber. Steep slopes indicate an open state, while low slopes indicate a closed state. Other recordings are shown in Supplementary Figs. 1–3. (B) The average ratios of the conductance at applied voltage (G) / maximum conductance (G_{max}). Current records were collected in response to more than 5 periods of triangular voltage waves. Data are means of more than 10 experiments (Supplementary Figs. 1–3) ± S.E. for each group. (C) Distribution of open state conductance of VDAC channels. Conductances were measured for 12 s under constant voltages at −50, −40, −30, −20, −10, +10, +20, +30, +40, +50 mV, respectively. The maximum conductance of each experiment was defined as the open state conductance. Histograms were constructed based on 52, 23, and 51 experiments for VDAC1, VDAC2, and VDAC3, respectively.

channel gating was activated in the presence of DTT (Fig. 4A upper panel). Clear open state and closed state were observed as in the cases of VDAC1 and VDAC2. The voltage-dependency also changed, becoming similar to those of VDAC1 and VDAC2 (Fig. 4B left panel). VDAC3 was closed at higher voltage in DTT-treated solution, suggesting that disulfide-bond formation blocks VDAC3 channel-gating.

To examine this hypothesis, we alkylated cysteine residues of VDAC3 with IAA to block disulfide-bond formation, and the activity of the alkylated VDAC3 was monitored in the absence of DTT. As expected, alkylation of thiols in VDAC3 caused activation of the gating (lower panel of Fig. 4A and right panel of Fig. 4B). These results indicate that disulfide-bond formation inactivated the gating of VDAC3, and suggest that VDAC3 function might be regulated by cysteine modification.

Since S-nitrosylation has been implicated in the regulation of the physiological functions of VDAC3, we next monitored the channel properties in the presence of GSNO, a direct nitric oxide (NO) donor for cysteine. As a result, clear channel gating of VDAC3 was observed in the presence of GSNO (Fig. 5). This further supports the idea that cysteine modification regulates VDAC3 functions.

3.4. Oxidation of recombinant VDAC3

To further confirm the disulfide-bond formation of VDAC3 under the conditions for the electrophysiological experiments, non-reducing SDS-PAGE analysis of the diluted VDAC3 samples containing various concentrations of DTT was performed after alkylation of thiols. A faster migrating band was observed for the VDAC3 in a solution with low concentration of DTT (Fig. 6A). With 0.01 mM of DTT, only faster migrating band was observed. A similar band was observed for VDAC3 treated with high concentration of H_2O_2 (Fig. 6B). Furthermore, the band shift was not observed when the H_2O_2-oxidized VDAC3 was treated with DTT before alkylation, indicating that the oxidation is reversible (Fig. 6C). These facts suggest that the faster migrating band would be the oxidized VDAC3 with intramolecular disulfide-bond, and the disulfide-bond would be easily formed by simple dilution of DTT.

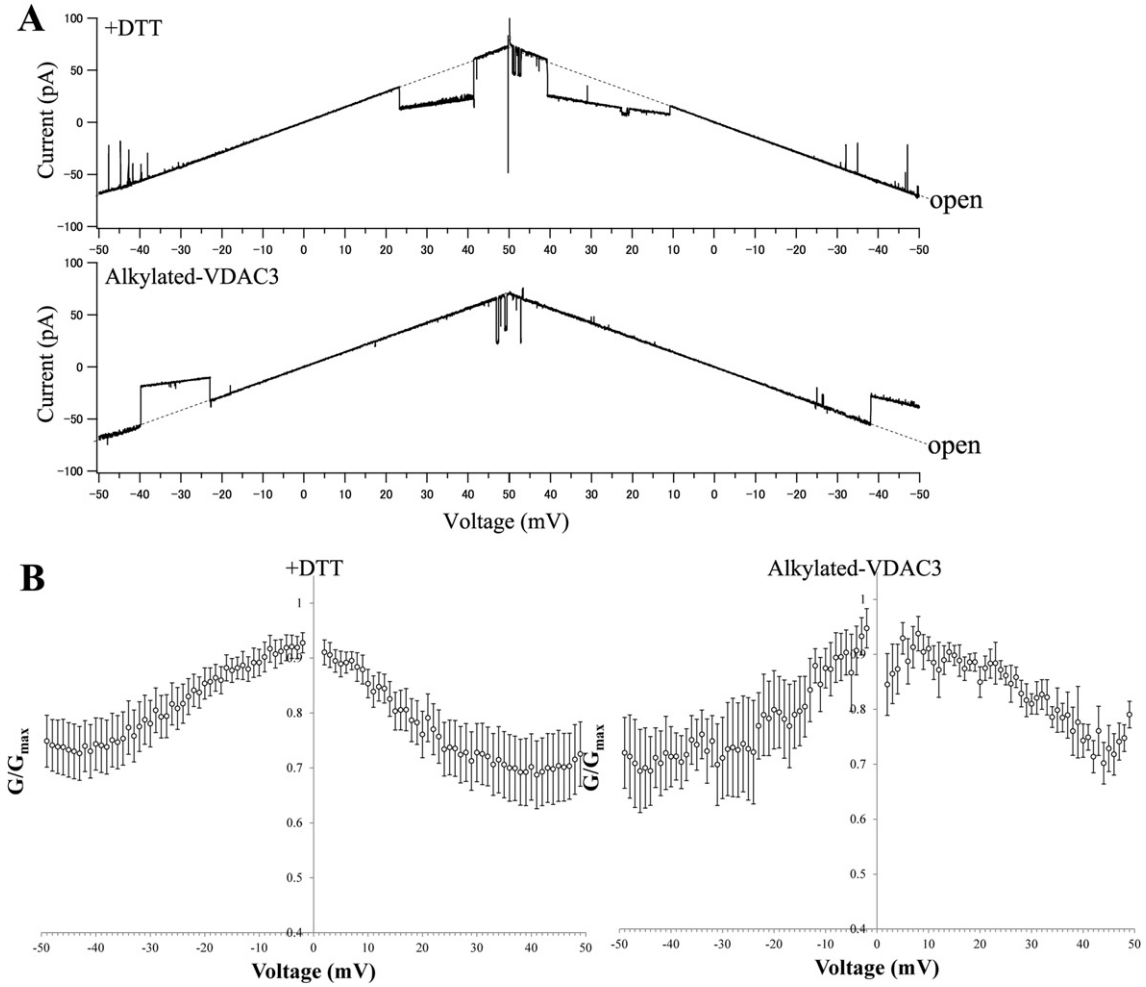

Fig. 4. Activation of VDAC3 by cysteine modification. (A) Current traces under triangular voltage waves (±50 mV, 0.5 kHz). Voltage-gating of VDAC3 in the presence of DTT (upper panel) was monitored. Voltage-gating of alkylated VDAC3 after pre-incubation with 1 μM IAA was monitored (lower panel). Final concentrations of VDAC-His_6 proteins were in a range of 0.1–10 ng/each chamber. (B) The ratios of the conductance at applied voltage (G) / maximum conductance (G_{max}). Current records were collected in response to more than 2 periods of triangular voltage waves. Data are means of more than 5 experiments ± S.E. for each group.

3.5. Analysis of VDAC3 cysteine mutants

The next question is, which cysteine residues are involved in the critical disulfide-bond formation? To address this question, we examined the channel gating properties of cysteine mutants of VDAC3. C122A and double cysteine mutant C2A/C8A clearly responded to linearly changing voltages, and showed clear open and closed conductance states (Fig. 7A). In contrast, the other single cysteine mutants C2A, C8A, C36A, C65A, and C229A showed weak responses, like VDAC3. Distinct bell-shaped voltage dependency was observed only for the C122A and C2A/C8A mutants (Fig. 7B). These results indicate that disulfide-bond formation of Cys122 with either Cys2 or Cys8 is critical for blocking voltage-dependent gating.

The homology model of VDAC3 constructed based on the reported crystal structure of VDAC1 indicated that Cys2 and Cys8 at the N-terminal region are positioned in close proximity to Cys122 at the bottom of the β-barrel (Fig. 8). This model suggests that the N-terminal region would be fixed at the bottom of the pore by disulfide-bond formation, causing inactivation of channel gating.

4. Discussion

The objective of this study was to clarify the molecular basis of the unique gating properties of VDAC3 by analyzing and comparing the channel properties of VDAC isoforms. Recombinant VDAC proteins corresponding to all three human isoforms were successfully expressed, purified, and refolded. The migration patterns of VDAC1 and VDAC3 in SDS-PAGE analysis were different, though the estimated molecular weights of VDAC1 and VDAC3 are almost the same. Yamamoto and colleagues also observed similar migration differences, although VDAC1 and VDAC2 have the same migration pattern [31]. Recombinant VDAC2-His_6 sequence in our study has extra-large N-terminal tag (2.5 kDa larger than native VDAC2), so the migration pattern of VDAC2 was slower than VDAC1. We speculated that structural modifications might exist in VDAC3 and indeed we found that disulfide-bond formation between N-terminal cysteine(s) and Cys122 occurred, as described above. It was also reported that artificial cross-linking of the N-terminal region and inner wall of VDAC1 by double cysteine mutation resulted in faster migration on SDS-PAGE [32]. We could observe the slower migrating band corresponding to the linearized form of VDAC3 only when thiols were alkylated to prevent disulfide formation, but not under commonly used electrophoresis conditions. It suggested that reduced form of VDAC3 is not stable and easily oxidized in the absence of high concentration of DTT. Hence, the observation that oxidized VDAC3 migrated faster than VDAC1 is consistent with the occurrence of disulfide-bond formation.

Electrophysiological study demonstrated that VDAC1 and VDAC2 had typical voltage-dependent gating activities. The voltage-response of VDAC2 was not as consistent as VDAC1 (Supplementary Figs. 1 and

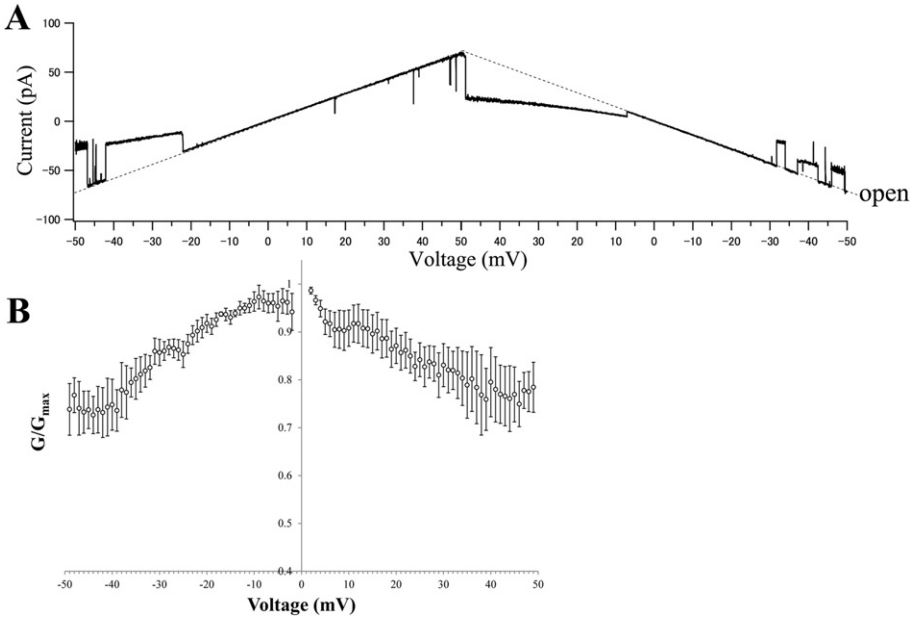

Fig. 5. Activation of VDAC3 by S-nitrosylation. (A) Current traces under triangular voltage waves (±50 mV, 0.5 kHz). Voltage-gating of VDAC3 in the presence of GSNO was monitored. Final concentrations of VDAC-His_6 proteins were in a range of 0.1–10 ng/each chamber. (B) The ratios of the conductance at applied voltage (G) / maximum conductance (G_{max}). Current records were collected in response to more than 9 periods of triangular voltage waves. Data are means of more than 4 experiments ± S.E. for each group.

2). Our recombinant VDAC2-His_6 protein has extra amino acid residues at N-terminal (Fig. 1), and this longer N-terminal might occasionally inhibit normal gating. Indeed, inflexible VDAC1 N-terminal region was reported to cause less response to voltage change [33].

VDAC1 contains 2 cysteines, and the cysteine functions on channel gating have been studied. It was reported that VDAC1 could exist in oxidized and reduced forms due to the cysteine modification status [34], although conductances of the oxidized and reduced forms of bovine VDAC1 reconstituted in planar bilayer membrane were similar. More recently, cysteine-less VDAC1 mutant was generated and investigated whether the cysteine residues are involved in its oligomerization and apoptosis [35]. No difference in the channel gating properties between native VDAC1 and the cysteine-less mutant was observed, and oligomer

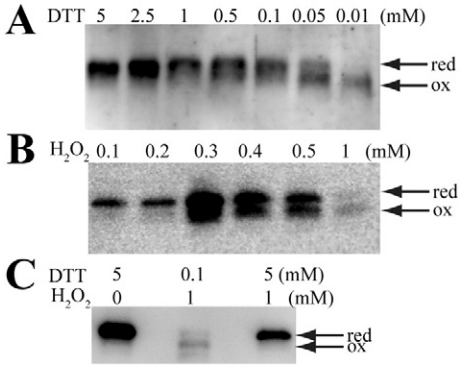

Fig. 6. Oxidation of VDAC3. (A) Oxidation by dilution of DTT to the indicated concentrations. The recombinant VDAC3-His_6 solution containing 5 mM DTT was diluted by an elution buffer without DTT (25 mM $NaPO_4$ (pH 7.0), 0.1 % LDAO, 1 M NaCl) and incubated at room temperature (RT) for 60 min. Then the remaining thiols were alkylated by the treatment with 100 μM IAA at RT for 10 min. The bands corresponding to the reduced state and the oxidized state are shown as "red" and "ox", respectively. (B) Oxidation by incubation with indicated concentrations of H_2O_2. The recombinant VDAC3-His_6 solution containing 0.1 mM DTT was incubated with the indicated final concentration of H_2O_2 at 30 °C for 30 min. (C) Reversible oxidation of VDAC3. Recombinant VDAC3-His_6 solution containing 0.1 mM DTT was treated with 1 mM H_2O_2 for 30 min (middle lane), or treated with 1 mM H_2O_2 for 30 min then with 5 mM DTT for 30 min (right lane). The left lane is the control sample stored in the solution containing 5 mM DTT.

formation was also not affected by the cysteine mutation. By now, cysteine function of VDAC1 has not been revealed.

VDAC2 contains as many as 9 cysteine residues and 2 of them positioned at the N-terminal region. The channel function and barrel stability of cysteine-less mutant of VDAC2 were studied [36,37]. The cysteine residues of VDAC2 were reported to mainly exist as free-thiol form and contributed barrel-lipid interaction. Channel gating property was slightly affected by the cysteine mutation. However, it was not yet known how the gating of VDAC2 regulates. It is interesting to evaluate its selectivity of the open and closed states by the response of reduced or oxidized condition.

On the other hand, the gating activity of VDAC3 was very weak, as previously reported for the human VDAC3 [38]. We found that channel gating of VDAC3 was activated by suppression of disulfide-bond formation, becoming similar to that of VDAC1 and VDAC2. Several proteins are known to form inter/intramolecular disulfide-bonds in response to redox signals, which thereby modulate their activities. For example, the tumor suppressor PTEN is reversibly inactivated by H_2O_2 and activated by DTT [39]. Cardiac calcium release channel (RyR1) and transient receptor potential cation channel (TRPA1) are activated by thiol oxidation and inactivated by DTT [40,41]. Channel gating of VDAC3 might be also controlled by redox signals, through disulfide-bond formation. It is well known that the cell cycle is regulated by cellular redox homeostasis [42,43]. By sensing such environmental change, VDAC3 might regulate physiological processes such as microtubule doublet formation in cycling cells and sperm. It was also reported that oxidative modification of thiol groups of VDAC caused loss of MMP [44]. Because VDAC3 was reported to be quantitatively the most important VDAC to sustain MMP in cancer cells [18], loss of MMP might be the result of inactivation of VDAC3. All of these findings are consistent with the idea that VDAC3 provides a redox-sensitive control mechanism for cellular activities, in contrast to the other VDAC isoforms.

It was reported that mouse VDAC3 did not insert easily into lipid membranes, but DTT aided its insertion [15]. In the case of human VDAC3, insertion was also hard to detect without addition of large amounts of DTT to the buffer solution. Detergent-solubilized VDAC could be spontaneously inserted [45] but its stability affected the insertion efficiency [46]. DTT may increase the structural stability of VDAC3

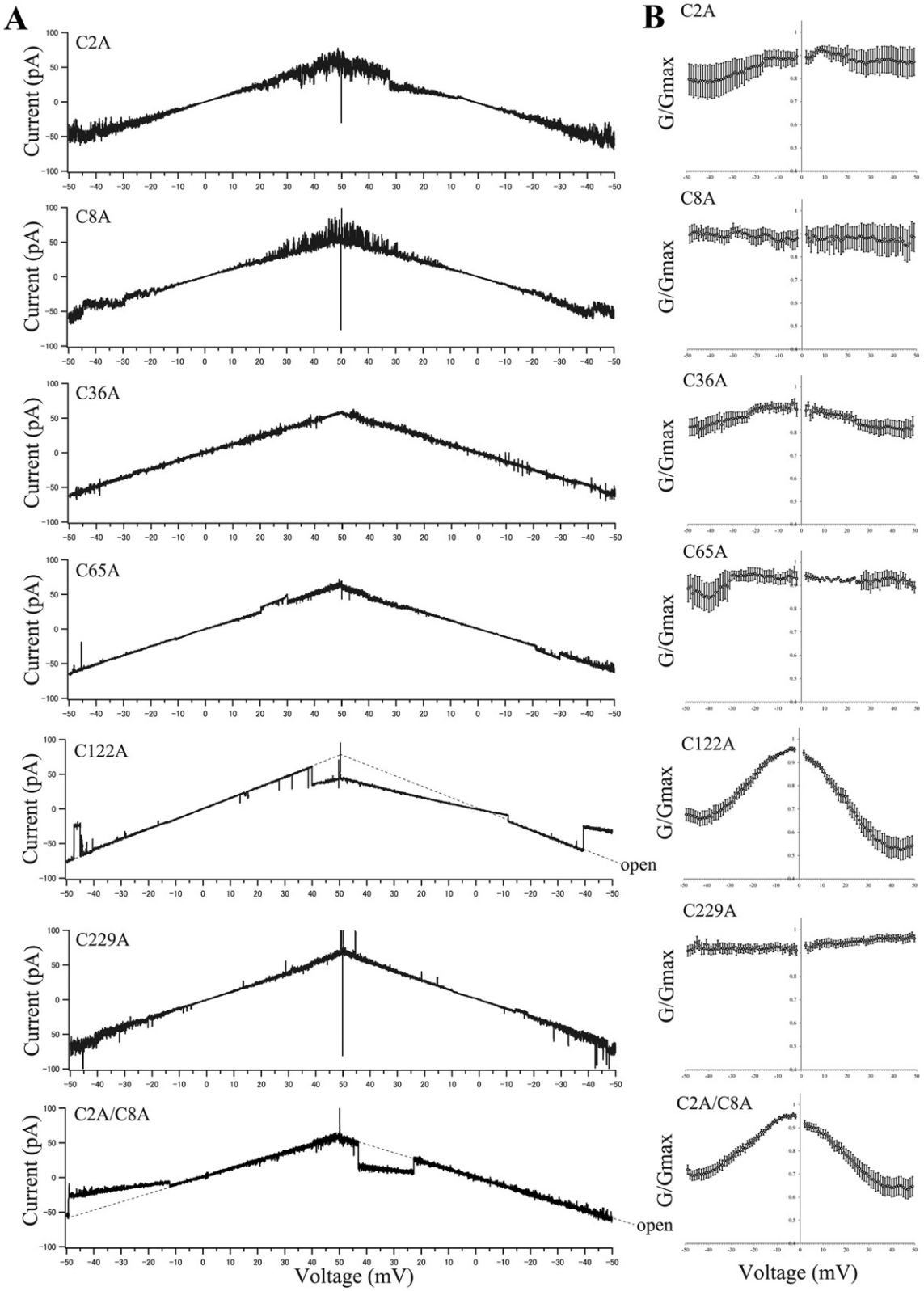

Fig. 7. Effect of mutation of various cysteine residues on voltage-gating of VDAC3. Voltage-gating of VDAC3 cysteine mutants was analyzed. Final concentrations of VDAC3-His_6 proteins were in a range of 0.1–10 ng/each chamber. (A) Current traces under triangular voltage waves (±50 mV, 0.5 kHz). (B) The ratios of the conductance at applied voltage (G) / maximum conductance (G_{max}). Current records were collected in response to more than 3 periods of triangular voltage waves. Data are means of more than 3 experiments ± S.E. for each group.

by preventing disulfide-bond formation, leading to an increase of insertion events.

Molecular structure of VDAC1 was solved by several researchers to be 19 β-barrel with an α-helix located within the pore [30,47,48]. Analysis of VDAC3 cysteine mutants revealed that disulfide-bond formation occurred between cysteine residues at the N-terminal region and at the bottom of the pore. It is established that the N-terminal region of VDAC3 is important for the channel properties [25], although

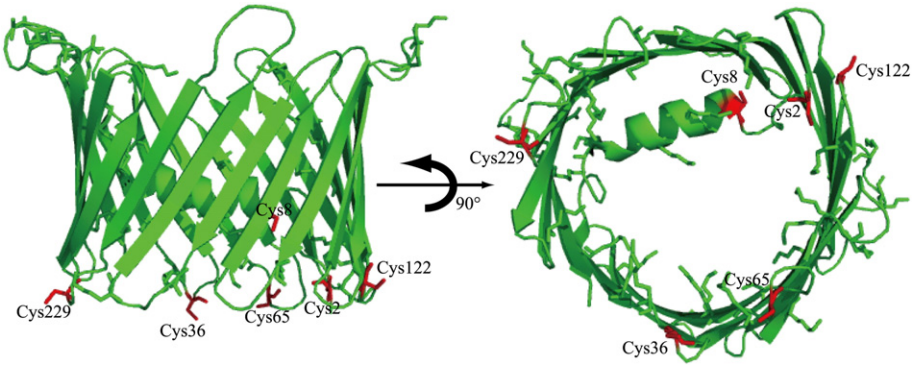

Fig. 8. Positions of cysteine residues of VDAC3, as predicted by homology modeling. Cysteine residues are shown in red. Cys2 and Cys8 are positioned at the N-terminal region and Cys36, Cys65, Cys122, and Cys229 are positioned at the bottom of the pore.

the reason for this was not determined. Further, the N-terminal region of VDAC1 is important for channel gating; voltage-gating of VDAC1 was not observed when the N-terminal region was removed [49–51] and cross-linking of the N-terminal region with the inner wall resulted in a constitutively open or closed state [32]. These findings are consistent with the idea that decreased channel gating of VDAC3 was due to fixation of the N-terminal region at the bottom of the pore. But the mechanism for open–closed transition by the translocation of the N-terminal region in the pore is still not clear. The closed state might be caused by the α-helix movement to inside of the pore, because the lower conductance state was often observed in normal VDAC3 channels, in which α-helix is likely to be fixed in the pore by disulfide bond. However, recent works using N-terminal deletion and double-cysteine mutants of VDAC1 suggested that α-helix would be located in the pore at the open state [32,51]. Further detailed researches of each VDAC subtype would be required to clarify how the N-terminal region regulates the gating of native VDACs.

Channel gating of VDAC3 was also activated by S-nitrosylation. Protein S-nitrosylation by NO has emerged as an important mechanism of cellular signal transduction and post-translational regulation. For example, protein kinase Bα (PKBα) is regulated by S-nitrosylation, which blocks disulfide-bond formation [52]. S-Nitrosylation of VDAC3 might also block disulfide-bond formation. Physiologically, VDAC3 is actually S-nitrosylated in spermatozoa [22]. S-Nitrosylation of VDAC3 may be important for sperm motility, because motility required both VDAC3 and NO signals [12,53]. In addition, S-nitrosylation of mitochondrial proteins potentiated VDAC-mediated Ca^{2+}-induced mitochondrial swelling and cytochrome c release [23]. S-Nitrosylated VDAC3 might function in such processes as the active form.

In conclusion, we examined the channel properties of the three human VDAC isoforms and found that the activity of VDAC3 is dependent upon the redox state of its cysteine residues. Our results indicate that VDAC3 activity may be regulated by redox sensing under physiological conditions — specifically by reversible disulfide-bond formation between cysteine residues located in the N-terminal region and at the bottom of the pore. It is noteworthy that VDAC3 has different functions in different muscle types, even though its expression levels are almost the same; VDAC3-deficient mice showed decreased affinity for ADP in heart but not in gastrocnemius muscle [54]. Thus, VDAC3 appears to have tissue-specific physiological roles. It would be interesting to examine whether redox sensing, post-translational modification or some other mechanism controls the activity of VDAC3 in specific cell types, tissues, or organs.

Competing financial interests

The authors declare no competing financial interests.

Transparency Document

The Transparency document associated with this article can be found, in the online version.

Acknowledgments

We thank the RIKEN BSI Research Resources Center for DNA sequence analysis. This work was partly supported by Grant-in-Aid for Scientific Research on Innovative Areas (Homeostatic regulation by various types of cell death) (26110004) from MEXT.

Appendix A. Supplementary data

Supplementary data to this article can be found online at http://dx.doi.org/10.1016/j.bbamem.2015.09.017.

References

[1] A. Messina, S. Reina, F. Guarino, V. De Pinto, VDAC isoforms in mammals, Biochim. Biophys. Acta 1818 (2012) 1466–1476.
[2] T. Hodge, M. Colombini, Regulation of metabolite flux through voltage-gating of VDAC channels, J. Membr. Biol. 157 (1997) 271–279.
[3] T. Rostovtseva, M. Colombini, VDAC channels mediate and gate the flow of ATP: implications for the regulation of mitochondrial function, Biophys. J. 72 (1997) 1954–1962.
[4] V. De Pinto, F. Guarino, A. Guarnera, A. Messina, S. Reina, F.M. Tomasello, V. Palermo, C. Mazzoni, Characterization of human VDAC isoforms: a peculiar function for VDAC3? Biochim. Biophys. Acta 1797 (2010) 1268–1275.
[5] R.A. Nakashima, P.S. Mangan, M. Colombini, P.L. Pedersen, Hexokinase receptor complex in hepatoma mitochondria: evidence from N,N'-dicyclohexylcarbodiimide-labeling studies for the involvement of the pore-forming protein VDAC, Biochemistry 25 (1986) 1015–1021.
[6] S. Shimizu, M. Narita, Y. Tsujimoto, Bcl-2 family proteins regulate the release of apoptogenic cytochrome c by the mitochondrial channel VDAC, Nature 399 (1999) 483–487.
[7] Y. Shi, J. Chen, C. Weng, R. Chen, Y. Zheng, Q. Chen, H. Tang, Identification of the protein–protein contact site and interaction mode of human VDAC1 with Bcl-2 family proteins, Biochem. Biophys. Res. Commun. 305 (2003) 989–996.
[8] K.D. Hinsch, V. De Pinto, V.A. Aires, X. Schneider, A. Messina, E. Hinsch, Voltage-dependent anion-selective channels VDAC2 and VDAC3 are abundant proteins in bovine outer dense fibers, a cytoskeletal component of the sperm flagellum, J. Biol. Chem. 279 (2004) 15281–15288.
[9] M. Colombini, A candidate for the permeability pathway of the outer mitochondrial membrane, Nature 279 (1979) 643–645.
[10] D. Neumann, J. Bückers, L. Kastrup, Two-color STED microscopy reveals different degrees of colocalization between hexokinase-I and the three human VDAC isoforms, PMC Biophys. 3 (2010) 4.
[11] M. Sampson, R. Lovell, D. Davison, W. Craigen, A novel mouse mitochondrial voltage-dependent anion channel gene localizes to chromosome 8, Genomics 36 (1996) 192–196.
[12] M.J. Sampson, W.K. Decker, A.L. Beaudet, W. Ruitenbeek, D. Armstrong, M.J. Hicks, W.J. Craigen, Immotile sperm and infertility in mice lacking mitochondrial voltage-dependent anion channel type 3, J. Biol. Chem. 276 (2001) 39206–39212.
[13] S. Majumder, M. Slabodnick, A. Pike, J. Marquardt, H.A. Fisk, VDAC3 regulates centriole assembly by targeting Mps1 to centrosomes, Cell Cycle 11 (2012) 3666–3678.
[14] S. Majumder, H. Fisk, VDAC3 and Mps1 negatively regulate ciliogenesis, Cell Cycle 12 (2013) 849–858.

[15] X. Xu, W. Decker, M.J. Sampson, W.J. Craigen, M. Colombini, Mouse VDAC isoforms expressed in yeast: channel properties and their roles in mitochondrial outer membrane permeability, J. Membr. Biol. 170 (1999) 89–102.
[16] S. Reina, A. Magrì, M. Lolicato, F. Guarino, A. Impellizzeri, E. Maier, R. Benz, M. Ceccarelli, V. De Pinto, A. Messina, Deletion of β-strands 9 and 10 converts VDAC1 voltage-dependence in an asymmetrical process, Biochim. Biophys. Acta 1827 (2013) 793–805.
[17] E.N. Maldonado, J.J. Lemasters, Warburg revisited: regulation of mitochondrial metabolism by voltage-dependent anion channels in cancer cells, J. Pharmacol. Exp. Ther. 342 (2012) 637–641.
[18] E.N. Maldonado, K.L. Sheldon, D.N. DeHart, J. Patnaik, Y. Manevich, D.M. Townsend, S.M. Bezrukov, T.K. Rostovtseva, J.J. Lemasters, Voltage-dependent anion channels modulate mitochondrial metabolism in cancer cells: regulation by free tubulin and erastin, J. Biol. Chem. 288 (2013) 11920–11929.
[19] A.M. Distler, J. Kerner, C.L. Hoppel, Post-translational modifications of rat liver mitochondrial outer membrane proteins identified by mass spectrometry, Biochim. Biophys. Acta 1774 (2007) 628–636.
[20] S. Zhao, W. Xu, W. Jiang, W. Yu, Y. Lin, T. Zhang, J. Yao, L. Zhou, Y. Zeng, H. Li, Y. Li, J. Shi, W. An, S.M. Hancock, F. He, L. Qin, J. Chin, P. Yang, X. Chen, Q. Lei, et al., Regulation of cellular metabolism by protein lysine acetylation, Science 327 (2010) 1000–1004.
[21] M. Yang, A. Camara, B. Wakim, Tyrosine nitration of voltage-dependent anion channels in cardiac ischemia-reperfusion: reduction by peroxynitrite scavenging, Biochim. Biophys. Acta 1817 (2012) 2049–2059.
[22] L. Lefièvre, Y. Chen, S.J. Conner, J.L. Scott, S.J. Publicover, W.C.L. Ford, C.L.R. Barratt, Human spermatozoa contain multiple targets for protein S-nitrosylation: an alternative mechanism of the. Modulation of sperm function by nitric oxide? Proteomics 7 (2007) 3066–3084.
[23] A.H.K. Chang, H. Sancheti, J. Garcia, N. Kaplowitz, E. Cadenas, D. Han, Respiratory substrates regulate S-nitrosylation of mitochondrial proteins through a thiol-dependent pathway, Chem. Res. Toxicol. 27 (2014) 794–804.
[24] Y. Sun, A.A. Vashisht, J. Tchieu, J.A. Wohlschlegel, L. Dreier, Voltage-dependent anion channels (VDACs) recruit Parkin to defective mitochondria to promote mitochondrial autophagy, J. Biol. Chem. 287 (2012) 40652–40660.
[25] S. Reina, V. Palermo, A. Guarnera, F. Guarino, A. Messina, C. Mazzoni, V. De Pinto, Swapping of the N-terminus of VDAC1 with VDAC3 restores full activity of the channel and confers anti-aging features to the cell, FEBS Lett. 584 (2010) 2837–2844.
[26] N. Yagoda, M. von Rechenberg, E. Zaganjor, A.J. Bauer, W.S. Yang, D.J. Fridman, A.J. Wolpaw, I. Smukste, J.M. Peltier, J.J. Boniface, R. Smith, S.L. Lessnick, S. Sahasrabudhe, B.R. Stockwell, RAS–RAF–MEK-dependent oxidative cell death involving voltage-dependent anion channels, Nature 447 (2007) 864–868.
[27] A.J. Bauer, S. Gieschler, K.M. Lemberg, A.E. McDermott, B.R. Stockwell, Functional model of metabolite gating by human voltage-dependent anion channel 2, Biochemistry 50 (2011) 3408–3410.
[28] P. Mueller, D. Rudin, H.T. Tien, W. Wescott, Reconstitution of cell membrane structure in vitro and its transformation into an excitable system, Nature 194 (1962) 979–980.
[29] A. Šali, T. Blundell, Comparative protein modelling by satisfaction of spatial restraints, J. Mol. Biol. 234 (1993) 779–815.
[30] R. Ujwal, D. Cascio, J.-P. Colletier, S. Faham, J. Zhang, L. Toro, P. Ping, J. Abramson, The crystal structure of mouse VDAC1 at 23 Å resolution reveals mechanistic insights into metabolite gating, Proc. Natl. Acad. Sci. U. S. A. 105 (2008) 17742–17747.
[31] T. Yamamoto, A. Yamada, M. Watanabe, Y. Yoshimura, N. Yamazaki, Y. Yoshimura, T. Yamauchi, M. Kataoka, T. Nagata, H. Terada, Y. Shinohara, VDAC1, having a shorter N-terminus than VDAC2 but showing the same migration in an SDS-polyacrylamide gel, is the predominant form expressed in mitochondria of various tissues, J. Proteome Res. 5 (2006) 3336–3344.
[32] B. Mertins, G. Psakis, W. Grosse, K.C. Back, A. Salisowski, P. Reiss, U. Koert, L.O. Essen, Flexibility of the N-terminal mVDAC1 segment controls the channel's gating behavior, PLoS One 7 (2012), e47938.
[33] S. Geula, D. Ben-Hail, V. Shoshan-Barmatz, Structure-based analysis of VDAC1: N-terminus location, translocation, channel gating and association with anti-apoptotic proteins, Biochem. J. 444 (2012) 475–485.
[34] V. De Pinto, J.A. al Jamal, R. Benz, G. Genchi, F. Palmieri, Characterization of SH groups in porin of bovine heart mitochondria. Porin cysteines are localized in the channel walls, Eur. J. Biochem. 202 (1991) 903–911.
[35] L. Aram, S. Geula, N. Arbel, V. Shoshan-Barmatz, VDAC1 cysteine residues: topology and function in channel activity and apoptosis, Biochem. J. 427 (2010) 445–454.
[36] S.R. Maurya, R. Mahalakshmi, Modulation of human mitochondrial voltage-dependent anion channel 2 (hVDAC-2) structural stability by cysteine-assisted barrel-lipid interactions, J. Biol. Chem. 288 (2013) 25584–25592.
[37] S.R. Maurya, R. Mahalakshmi, Cysteine residues impact the stability and micelle interaction dynamics of the human mitochondrial β-barrel anion channel hVDAC-2, PLoS ONE 9 (2014), e92183.
[38] V. Checchetto, S. Reina, A. Magrì, I. Szabo, V. De Pinto, Recombinant human voltage dependent anion selective channel isoform 3 (hVDAC3) forms pores with a very small conductance, Cell. Physiol. Biochem. 34 (2014) 842–853.
[39] S. Lee, K. Yang, C. Lee, W. Jeong, J. Kwon, S.G. Rhee, Reversible inactivation of the tumor reversible inactivation of the tumor suppressor PTEN by H_2O_2, J. Biol. Chem. 277 (2002) 20336–20342.
[40] B. Aghdasi, M. Reid, S. Hamilton, Nitric oxide protects the skeletal muscle Ca^{2+} release channel from oxidation induced activation, J. Biol. Chem. 272 (1997) 25462–25467.
[41] N. Takahashi, T. Kuwaki, S. Kiyonaka, T. Numata, D. Kozai, Y. Mizuno, S. Yamamoto, S. Naito, E. Knevels, P. Carmeliet, T. Oga, S. Kaneko, S. Suga, T. Nokami, J. Yoshida, Y. Mori, TRPA1 underlies a sensing mechanism for O_2, Nat. Chem. Biol. 7 (2011) 701–711.
[42] E.H. Sarsour, A.L. Kalen, Z. Xiao, T.D. Veenstra, L. Chaudhuri, S. Venkataraman, P. Reigan, G.R. Buettner, P.C. Goswami, Manganese superoxide dismutase regulates a metabolic switch during the mammalian cell cycle, Cancer Res. 72 (2012) 3807–3816.
[43] A. Kim, W. Zhong, T.D. Oberley, Reversible modulation of cell cycle kinetics in NIH/3T3 mouse fibroblasts by inducible overexpression of mitochondrial manganese superoxide dismutase, Antioxid. Redox Signal. 6 (2004) 489–500.
[44] U. Saeed, L. Durgadoss, R.K. Valli, D.C. Joshi, P.G. Joshi, V. Ravindranath, Knockdown of cytosolic glutaredoxin 1 leads to loss of mitochondrial membrane potential: implication in neurodegenerative diseases, PLoS One 3 (2008), e2459.
[45] M. Zizi, L. Thomas, E. Blachly-Dyson, M. Forte, M. Colombini, Oriented channel insertion reveals the motion of a transmembrane beta strand during voltage gating of VDAC, J. Membr. Biol. 144 (1995) 121–129.
[46] S.R. Maurya, R. Mahalakshmi, Influence of protein-micelle ratios and cysteine residues on the kinetic stability and unfolding rates of human mitochondrial VDAC-2, PLoS One 9 (2014), e87701.
[47] M. Bayrhuber, T. Meins, M. Habeck, S. Becker, K. Giller, S. Villinger, et al., Structure of the human voltage-dependent anion channel, Proc. Natl. Acad. Sci. U. S. A. 105 (2008) 15370–15375.
[48] S. Hiller, R.G. Garces, T.J. Malia, V.Y. Orekhov, M. Colombini, G. Wagner, Solution structure of the integral human membrane protein VDAC-1 in detergent micelles, Science 321 (2008) 1206–1210.
[49] D.A. Koppel, K.W. Kinnally, P. Masters, M. Forte, E. Blachly-dyson, C.A. Mannella, Bacterial expression and characterization of the mitochondrial outer membrane channel, J. Biol. Chem. 273 (1998) 13794–13800.
[50] S. Abu-Hamad, N. Arbel, D. Calo, L. Arzoine, A. Israelson, N. Keinan, R. Ben-Romano, O. Friedman, V. Shoshan-Barmatz, The VDAC1 N-terminus is essential both for apoptosis and the protective effect of anti-apoptotic proteins, J. Cell Sci. 122 (2009) 1906–1916.
[51] U. Zachariae, R. Schneider, R. Briones, β-barrel mobility underlies closure of the voltage-dependent anion channel, Structure 20 (2012) 1–10.
[52] X.-M. Lu, M. Lu, R.G. Tompkins, A.J. Fischman, Site-specific detection of S-nitrosylated PKB alpha/Akt1 from rat soleus muscle using CapLC-Q-TOF(micro) mass spectrometry, J. Mass Spectrom. 40 (2005) 1140–1148.
[53] S.E. Lewis, E.T. Donnelly, E.S. Sterling, M.S. Kennedy, W. Thompson, U. Chakravarthy, Nitric oxide synthase and nitrite production in human spermatozoa: evidence that endogenous nitric oxide is beneficial to sperm motility, Mol. Hum. Reprod. 2 (1996) 873–878.
[54] K. Anflous-Pharayra, N. Lee, D.L. Armstrong, W.J. Craigen, VDAC3 has differing mitochondrial functions in two types of striated muscles, Biochim. Biophys. Acta 1807 (2011) 150–156.